Renal cell carcinoma: real-time contrast-enhanced ultrasound findings

Zuo-Feng Xu, Hui-Xiong Xu, Xiao-Yan Xie, Guang-Jian Liu, Yan-Ling Zheng, Jin-Yu Liang, Ming-De Lu

Department of Medical Ultrasonics, The First Affiliated Hospital, Institute of Diagnostic and Interventional Ultrasound, Sun Yat-Sen University, 58 Zhongshan Rd 2, Guangzhou 510080, China

Abstract

Objective: To investigate the findings of renal cell carcinomas (RCCs) on contrast-enhanced ultrasound (CEUS).
Methods: CEUS features of 84 RCCs confirmed by pathologic examination in 81 patients were retrospectively analyzed. A contrast-specific mode and a sulfur hexafluoride-filled microbubble contrast agent were used for CEUS. The enhancement pattern, extent, and dynamic change in the cortical, corticomedullary, and late phases were evaluated.
Results: On CEUS, the emergence of tumor enhancement was earlier in two nodules (2.4%), simultaneous in 71 (84.5%), and later in 11 (13.1%), in comparison with the adjacent renal cortex. Seventy-four RCC nodules (88.1%) showed hyper-enhancement ($n = 2$) or iso-enhancement ($n = 72$) during the cortical phase, and the remaining 10 (11.9%) showed hypo-enhancement. Twenty-three nodules (27.4%) showed homogeneous enhancement and 61 (72.6%) inhomogeneous enhancement. In the corticomedullary phase, the nodules showed hypo-enhancement in 68 (81.0%) and iso-enhancement in 16 (19.0%). In the late phase, all RCCs showed the same enhancement pattern as that shown in the corticomedullary phase. Seventy-two (85.7%) nodules showed a clear perilesional rim-like enhancement in late phase.
Conclusions: Hyper- or iso-enhancement during the cortical phase, subsequent washout in late phase, inhomogeneous enhancement, and perilesional rim-like enhancement are clues for RCCs, which might be useful for characterization of RCCs.

Key words: Contrast-enhanced ultrasound—Kidney—Focal renal lesion—Renal cell carcinoma—Ultrasound

Correspondence to: Hui-Xiong Xu; *email:* xuhuixiong@hotmail.com

Renal cell cancer (RCC) is the fifth most common cancer in men, and the most common malignant tumor of kidney, which accounts for 80% to 90% of renal tumors. Preoperative imaging modalities such as ultrasound (US), computed tomography (CT), and magnetic resonance imaging (MRI) have been widely used to confirm the diagnosis and provide important information for the planning and determination of the surgical approach and strategy [1, 2]. US is a real-time, easy accessible, cost-effective, and non-invasive imaging modality; however, its use in clinic is limited because of its low sensitivity in the detection and characterization of many parenchymal lesions in kidneys. Contrast-enhanced CT or MRI is more often required for differentiation diagnosis between some malignant and benign lesions [3]. Recently, the development of ultrasound contrast agent (UCA) and contrast-specific imaging technique have enabled contrast-enhanced ultrasound (CEUS), a novel imaging modality for wide use in many solid organs such as liver. CEUS allows continuous observation of intralesional micro- and macro-circulation, which may also be useful in diagnosis of focal lesions in the kidney, although the blood supply of renal masses is completely different from that of liver masses. In addition, given the fact that UCAs are relatively harmless with a low incidence of side effect and not nephrotoxic, CEUS can be used in patients with iodine allergy and impaired renal function that may be contraindications to contrast-enhanced CT or MRI [4]. Although potentially a very useful imaging tool, CEUS is still not widely used in the evaluation of renal tumors [5–7]. This study aimed to investigate the imaging findings of RCCs on CEUS.

Materials and methods

Patients

Between September 2004 and June 2008, 152 consecutive patients with 166 focal renal lesions that were firstly

detected by baseline US underwent CEUS in our department. Among them, 81 patients with 84 RCCs were retrospectively included in the study. The inclusion criteria were: (1) aged 18–80 years; (2) identified as solid lesion on baseline US; (3) histopathological confirmation of RCC. The other 71 patients were excluded because of the following reasons: (1) having no definite final diagnoses ($n = 10$); (2) having other final diagnoses ($n = 61$), including renal angiomyolipoma in 25, renal metastasis in 6, complex cyst in 10, Bertin's column in 7, renal pelvic carcinoma in 4, renal abscess in 6, Wilm's tumor in 1, renal adenoma in 1, and malignant lobus intermedius tumor in 1.

The final diagnoses of the 84 RCC lesions were all confirmed by histopathological examination with specimen obtained from surgery. They were 65 (77.4%) clear cell carcinomas, 9 (10.7%) papillary carcinomas, 4 (4.8%) chromophic cell carcinomas, 5 (6.0%) mixed cell carcinomas, and 1 (1.1%) chromophobe cell carcinoma. The patients were 59 (72.8%) men and 22 (27.2%) women with a mean age ± SD of 46.6 ± 13.1 years (range, 22–76 years). Patients with serious cardio-pulmonary diseases, pregnancy or lactation were excluded from this study. Informed consent was obtained from all patients, and the study was approved by the institutional ethical committee.

Seventy-eight patients had single nodule in each and three patients had two nodules in each. In patients with multiple nodules, each nodule visualized on baseline US was selected for CEUS evaluation one after another at about 6–10 min interval from the previous contrast agent injection, until the clearance of microbubble in the blood vessels. Therefore, a total of 84 nodules were observed, their mean diameter measured on US was 4.2 ± 2.2 cm (range, 1.5–11.7 cm). Among them, 38 nodules were ≤3.0 cm in maximum diameter and 46 nodules were >3.0 cm.

UCA

The UCA used in this study was SonoVue (Bracco, Milan, Italy), a sulfur hexafluoride (SF6)-filled microbubble contrast agent that is stabilized by phospholipids. The diameters of microbubbles were <8 μm (mean 2–3 μm). Before use, 5 mL of 0.9% sodium chloride solution was injected into the bottle, and then the bottle was shaken until the powder and solvent were completely dispersed. Through a 20-gauge intravenous cannula, 2.4 mL of SonoVue was injected into the antecubital vein with a bolus fashion per injection, followed by a flush of 5 mL 0.9% sodium chloride solution.

Baseline US and CEUS examination

The US equipment used in this study was an Acuson Sequoia 512 scanner (Siemens Medical Solutions, Mountain View, CA) with a 4V1 vector transducer that had a frequency range of 1.0–4.0 MHz. A contrast-specific imaging mode of contrast pulse sequencing (CPS) (Siemens Medical Solutions) was available with the machine. The CPS technique allows continuous low-mechanical index (MI) imaging with a high microbubble-tissue ratio [8, 9]. The range of the MI value shown on the screen was 0.15–0.21.

Baseline US was initially performed to scan the tumor-bearing kidney. The location, size, echogenicity, shape, and margin of the tumors were recorded. Then the tumor was targeted, and the imaging settings such as gain, depth, and focal zone were optimized to ensure enough image quality. Generally, a single focal zone was placed at the bottom of the lesion. Color or power Doppler sonography was performed to evaluate the intratumoral vascularity, and Doppler spectral analysis of intratumoral vessels was performed to identify pulsatile arterial or continuous venous flow. Afterward, the CPS function was initiated. The imaging settings were readjusted to locate the targeted tumor in the center of the screen, and focus was placed at the bottom of it. The tumor and the adjacent tissue were observed continuously for at least 3 min. The timer was started at the moment of intravenous injection of UCA administration. The vascular phase of CEUS was classified into cortical (8–15 s to 30–35 s after UCA injection), corticomedullary (36–41 s to 120 s), and late (>120 s to the disappearance of bubble) phases according to the literatures [4, 5, 7]. Digital cine clips of typical baseline US images and the whole process of CEUS images were stored in the hard disk incorporated in the scanner for subsequent analysis. All the US examinations were performed by one of two experienced investigators.

Image analysis

Digital cine clips of baseline US and CEUS images of the 84 RCCs were retrospectively analyzed in consensus by two readers. The parameters described below were evaluated and recorded: tumor enhancement extent, pattern, and their dynamic change along with the CEUS process, as well as other special changes during enhancement. The differences in initial enhancement and enhancement extent between the tumor and the peripheral renal cortex were compared. The enhancement patterns of the tumors were classified as follows: no enhancement—no appearance of microbubble signals in the lesion; homogeneous enhancement—diffuse lesion enhancement with the same level; and inhomogeneous enhancement—lesion enhancement with different levels [10]. In comparison with the adjacent renal cortex, the enhancement extent of the tumor was classified as hyper-enhancement, iso-enhancement, hypo-enhancement, and non-enhancement [5]. The so-called pseudo-capsule enhancement in CEUS was defined as rim-like enhancement around the tumor, which became more distinct in the late phase [11].

Statistical analysis

The statistical analysis was performed using the SPSS 10.0 software package (SPSS Inc., Chicago, IL). Continuous data are expressed as mean ± SD. An independent-sample *t*-test was applied to compare the differences in the enhancement time between RCC and the adjacent renal parenchyma. The Fisher exactor χ^2 test was used to compare difference in terms of enhancement pattern, homogeneity of tumor enhancement, and perilesional rim-like enhancement on CEUS. A two-tailed *P* value of less than 0.05 was considered statistically significant.

Results

On baseline US, 44 (52.4%) of the 84 observed nodules were located in the left kidneys, and 40 (47.6%) were in the right sides. The numbers of lesions that located in the upper pole, middle portion, and inferior pole of kidneys were 22(26.2%), 32(38.1%), 30(35.7%), respectively. Fourteen lesions (16.7%) were irregularly shaped and poorly demarcated from the adjacent tissue, and the remaining 70 (83.3%) were ovoid and well circumscribed. The numbers of lesions that showed hypoechogenicity, isoechogenicity, and hyperechogenicity were 34 (40.5%), 22 (26.2%), and 28 (33.3%), respectively. Only 34 lesions (40.5%) showed intralesional flow signals on Color Doppler ultrasound, the mean maximum velocity of which was 43.9 ± 15.3 cm/s (range, 24.8–95.0 cm/s), and the mean resistance index (RI) was 0.65 ± 0.13 (range, 0.52–0.83).

On CEUS, the time interval between the start of contrast agent injection and the initial enhancement of renal cortex and that between the start of contrast agent injection and initial enhancement of RCC were 11.8 ± 3.3 s (range, 6–23 s) and 12.2 ± 3.2 s (range, 6–24 s) respectively ($P > 0.05$). Compared with the adjacent renal cortex, the numbers of the lesions that showed earlier enhancement, simultaneous enhancement, and later enhancement were 2 (2.4%), 71 (84.5%), 11 (13.1%), respectively.

During the cortical phase, 74 (88.1%) tumors showed hyper-enhancement ($n = 2$) or iso-enhancement ($n = 72$), while the other 10 (11.9%) showed hypo-enhancement. Enhancement patterns of RCCs were homogeneous in 23 (27.4%) nodules and inhomogeneous in 61 (72.6%). As to the 61 RCCs that showed inhomogeneous enhancement, 1 showed nonenhancement at the central portion and a thick rim-like enhancement was seen at the peripheral portion of the nodule (Fig. 1). Non-enhanced areas were observed at both the peripheral and central portions in the other 60 nodules (Fig. 2).

In the corticomedullary phase, the hyper- or iso-enhanced areas in 58 (73.4%) of the 74 nodules in cortical phase faded out gradually and were visualized as hypo-enhancement in comparison with the adjacent renal

parenchyma (Fig. 3). The contours of these lesions became more clear during this phase. The remaining 16 (26.6%) of the 74 nodules that showed hyper- or iso-enhancement in cortical phase were still hyper- or iso-enhanced in this phase. The other 10 nodules that showed hypo-enhancement during the cortical phase continued to be hypo-enhancement during the corticomedullary phase.

In the late phase, the signals of microbubbles within both renal parenchyma and the lesions became weak. And, all RCC lesions showed the same enhancement patterns as those observed in the corticomedullary phase.

In 72 (85.7%) of 84 nodules, thin rim-like enhancement around the tumors was observed throughout the various vascular phases. During the cortical phase, the peritumoral rims were hyper-enhancing or iso-enhancing, whereas in the corticomedullary and late phases, the rims all became hyper-enhancing in comparison with the adjacent renal parenchyma, which made the boundary of the tumor more distinct (Fig. 4). Among them, 51 lesions (70.8%) showed complete peritumoral rim-like enhancement and the remaining 21 lesions (28.2%) showed incomplete peritumoral rim-like enhancement.

The CEUS findings in relationship with the different histological subtypes and tumor sizes were summarized in Tables 1 and 2 respectively. In comparison with clear cell carcinomas, subtype of papillary carcinoma tended to exhibit hypo-enhancement and homogeneous enhancement during the cortical phase (Table 1). On the other hand, tumors > 3.0 cm in diameter was apt to demonstrate inhomogeneous enhancement compared with those ≤3.0 cm (Table 2).

Discussion

RCC is characterized by numerous thin-walled blood vessels with rich blood flow pathologically [6, 12], and intratumoral necrosis, hemorrhage, and calcification are common [12]. Almost 83% of asymptomatic tumors were detected by baseline US [1, 2]; however, US has low ability to show the microvascularity in RCCs and the echogenicity on US has not been adequate enough to make use for characterization. Forman et al. [13] showed that 77% of small RCCs presented variable degrees of echogenicity and 32% were hyperechoic so as to mimic renal angioleiomyolipomas (RAMLs). Conversely, Jinzaki et al. [14] reported that RAMLs containing a small amount of fat often appear as iso- or moderately hyperechoic on US. Therefore, solely depending on the echogenicity on US cannot reliably differentiate these two entities, and further imaging examination such as CT or MRI is necessary [3, 15]. Evaluation of tumor vascularity is particularly important for their characterization [6]. Conventional color Doppler US has low ability in depicting the intratumoral vascularity, as shown in this series flow signals were detected only in 41% RCCs.
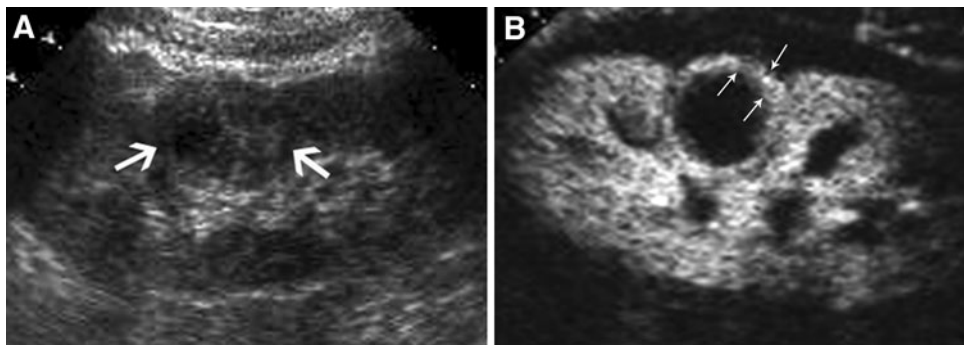
Fig. 1. Renal clear cell carcinoma in a 48-year-old man. **A** Baseline ultrasound shows a poorly demarcated iso-echoic solid nodule (*large arrows*) sized 2.5 cm in the middle of the right kidney, no obviously anechoic area is found in the nodule. **B** Contrast-enhanced ultrasound obtained during the cortical phase (19 s after contrast agent administration) shows a round and smooth nonenhancing area at the central portion, and a thick regular rim-like iso-enhancement (*small arrows*) at the periphery portion of the nodule. Final pathological examination revealed the nonenhancement at the central portion is related with necrosis instead of cyst or fluid.
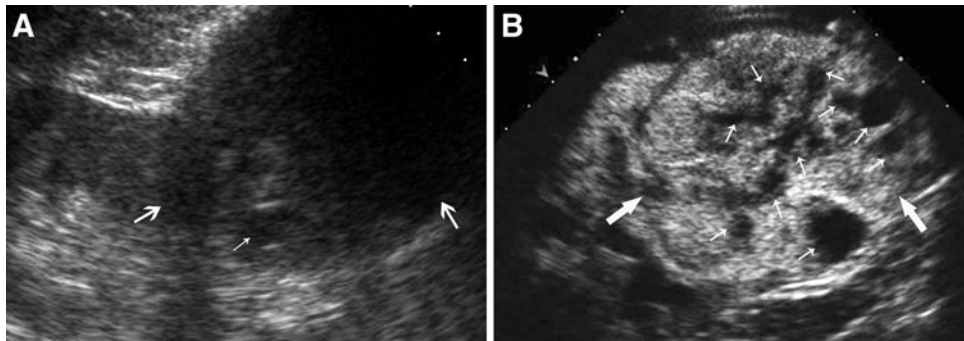

Fig. 2. Renal clear cell carcinoma in a 43-year-old man. **A** Baseline ultrasound shows a poorly demarcated iso-echoic nodule (*large arrows*) sized 5.4 cm in the inferior pole of the right kidney. An ambiguous anechoic area (*small arrow*) is found in the bottom of the nodule. **B** The nodule shows inhomogeneous non-enhancement (*small arrows*) at both the central and periphery portion during the cortical phase (19 s after contrast agent administration) of CEUS.
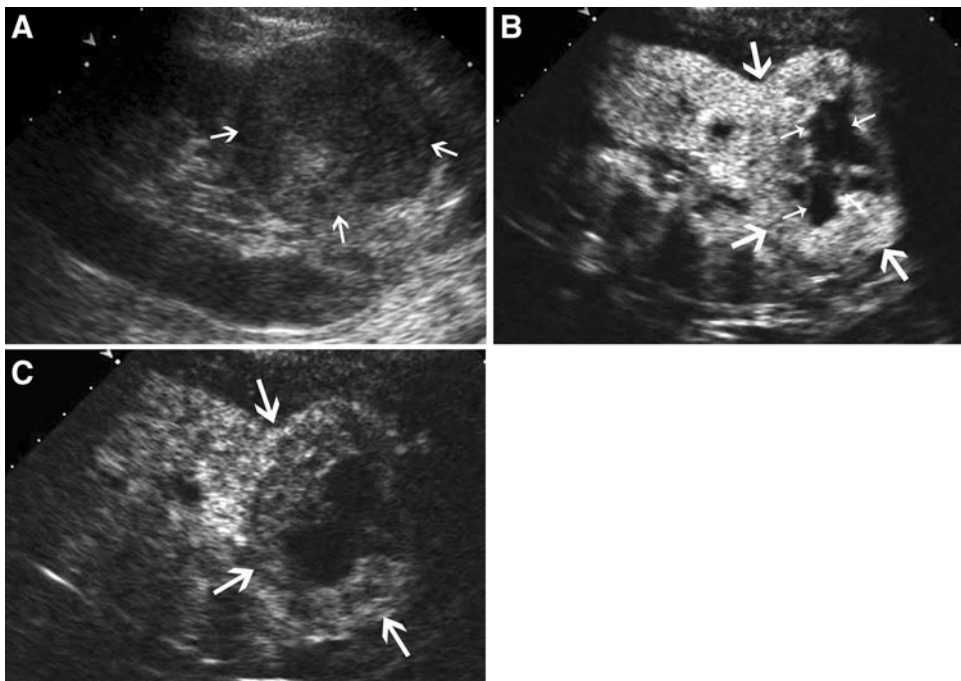

Fig. 3. Renal clear cell carcinoma in a 38-year-old man. **A** Baseline ultrasound shows a well-demarcated iso-echoic nodule (*large arrows*) sized 5.3 cm in the inferior pole of the left kidney. **B** During the cortical phase (21 s after contrast agent administration) of CEUS, the nodule shows inhomogeneous iso-enhancement, and irregular nonenhancement (*small arrows*) is observed in the nodule. **C** The enhancement fades out, and the nodule (*arrows*) shows hypo-enhancement during the corticomedullary phase (48 s after contrast agent administration).
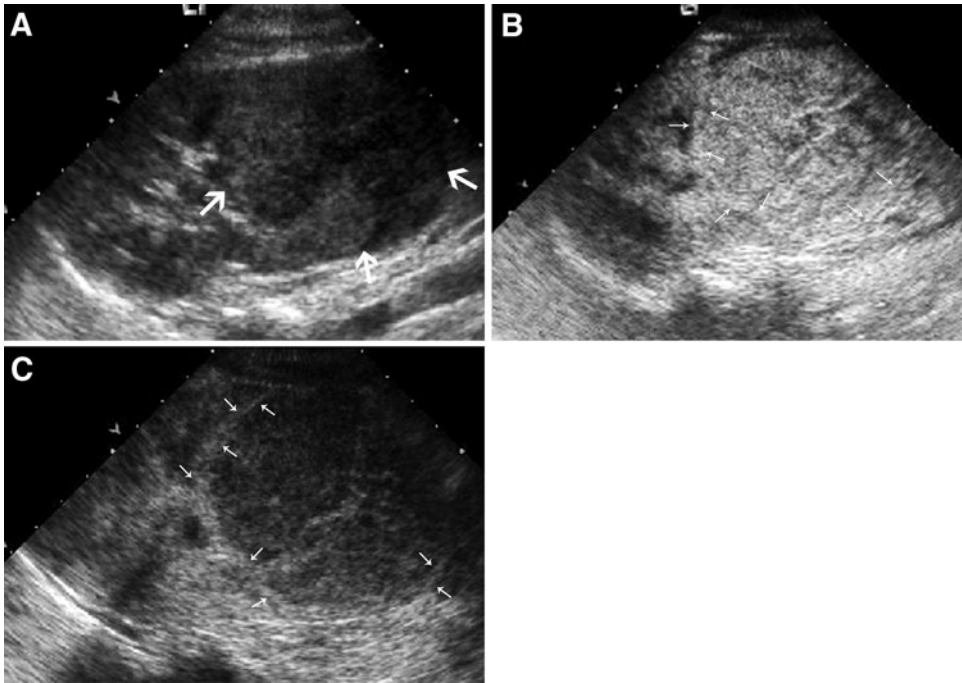
Fig. 4. Renal clear cell carcinoma in a 48-year-old man. **A** Baseline ultrasound shows a poorly demarcated iso-echoic nodule (*large arrows*) sized 6.1 cm in the inferior pole of the left kidney. **B** A thin enhanced rim (*small arrows*) of peritumoral tissue is observed in the nodule in the cortical phase (25 s after contrast agent administration). **C** The rim is better seen in the late phase (129 s after contrast agent administration).

Table 1. CEUS findings of different histological subtypes in 84 renal cell carcinomas

Histological subtype	n	Hyper- or iso-enhanced in cortical phase (%)	Washout in late phase (%)	Inhomogeneous enhancement (%)	Perilesional rim-like enhancement (%)
Clear cell carcinoma	65	92.3 (60/65)	78.3 (47/60)	80.0 (52/65)	89.2 (58/65)
Papillary carcinoma	9	44.4 (4/9)[a]	75.0 (3/4)	33.3 (3/9)[a]	77.8 (7/9)
Chromophic cell carcinoma	4	100 (4/4)	75.0 (3/4)	50.0 (2/4)	50.0 (2/4)
Mixed cell carcinomas	5	100 (5/5)	80.0 (4/5)	80.0 (4/5)	80.0 (4/5)
Chromophobe cell carcinoma	1	100 (1/1)	100 (1/1)	0 (0/1)	100 (1/1)

[a] In comparison with clear cell carcinoma, $P < 0.01$

Table 2. CEUS findings in relationship with tumor size in 84 renal cell carcinomas

Tumor diameter	n	Hyper- or iso-enhanced in cortical phase (%)	Washout in late phase (%)	Inhomogeneous enhancement (%)	Perilesional rim-like enhancement (%)
≤3 cm	38	84.2 (32/38)	71.8 (23/32)	55.3 (21/38)	78.9 (30/38)
>3 cm	64	91.3 (42/46)	83.3 (35/42)	86.9 (40/46)[a]	91.3 (42/46)

[a] In comparison with tumors ≤3 cm, $P < 0.01$

CEUS can provide better assessment of vascular morphology and enhancement pattern since in allows evaluation of both miro- and macro-circulation of the tumors, thus it has potential to improve the detection and characterization of RCCs. Unlike the contrast agents used in CT and MRI, US contrast agents are blood pool agents; because the microbubbles do not diffuse through the vascular endothelium into the interstitium, hence lead to more reliable depiction of the vascularity of tumors [8, 16, 17]. Most importantly, UCAs have no reported side effects on the kidneys in human beings to date [4]. It has been proven that CEUS is helpful to differentiate renal pseudotumors from true renal masses, and CEUS is better than CECT in showing intralesional vascularity, tumoral pseudocapsule, and tumor vascularity in the septa of cystic renal masses [5–8, 18–21].

As to CEUS for RCC, some investigators believed that CEUS could show more characteristic features of RCCs, and it could improve detection and characterization of renal masses [6, 22–24]. Using a high-MI CEUS technique and Levovist (SH U 508A; Schering AG, Berlin, Germany), Tamai et al. [6] found tumor blood flow in all 29 patients with renal lesions, while contrast CT failed to show in 5 patients, and among clear cell carcinomas, hypervascularity on CEUS was observed in 17 of 18 patients. Using a low-MI CEUS technique and SonoVue, Yang et al. [22] found that 76 of 98 (78%) renal clear cell carcinomas showed a wash-in

and wash-out pattern of enhancement, and 58 of 98 (59%) showed pseudocapsule enhancement. Compared to Yang's results, in this series, CEUS also showed that 92% of renal clear cell carcinomas were hyper- or iso-enhancement in the cortical phase, and wash-out in the late phase was found in 78% tumors. However, perilesional rim-like enhancement was shown in more (89%) lesions. Besides that, the CEUS findings in relationship with pathological subtypes were evaluated in this study. In contrast to the hyper-vascularity generally found in clear cell carcinomas, papillary carcinoma tended to exhibit hypo-enhancement and homogeneous enhancement during the cortical phase. Mixed cell carcinomas in this study had the component of clear cell carcinoma, so they also exhibited hyper-vascularity during cortical phase. And no matter what subtypes it was, inhomogeneous enhancement and pseudocapsule enhancement were the major findings for RCCs.

The thin rim-like enhancement around the tumor might represent the tumoral pseudocapsule, which is resulted from tumor growth producing compression, ischemia, and necrosis to adjacent normal parenchyma, with subsequent deposition of fibrous tissue, and usually associated with low histological grade RCC [25–27]. The presence of a pseudocapsule is considered a useful sign for discriminating RCCs, and it may be a criterion for nephronsparing surgery [28]. In addition, almost 73% of RCCs were inhomogeneous enhanced, and nonenhanced areas could be found in the inhomogeneous enhanced nodules. The nonenhanced areas might represent the necrosis and hemorrhage within the tumor, the detection rate of which increased with tumor growth. As shown in this series, tumors >3.0 cm in diameter was apt to demonstrate inhomogeneous enhancement compared with those ≤3.0 cm.

Despite of the characteristic findings of RCCs on CEUS revealed in this series, some investigators believed that RCCs had no particularly typical CEUS pattern and demonstrated some overlapping with the appearance of other renal masses [29, 30]. Haendl et al. [29] examined 30 patients with solid renal tumors before surgery with CEUS using the microbubble contrast agent SonoVue. They considered that RCCs showed chaotic vascularization in CEUS without typical vascularization patterns. However, only 25 RCCs, 2 urothelial carcinomas, and 3 oncocytomas were included in their study; thus, the results had no universality. Quaia et al. [30] examined 26 patients with 26 renal masses by using pulse inversion harmonic imaging with Levovist. They found that the differential diagnosis both in solid and in cystic renal masses still remains difficult with CEUS. Therefore, further studies with a larger sample size and including other types of renal lesions are mandatory to validate the results in this series.

The kidney enhances quickly and intensely after UCA injection due to the abundant blood flow. Afterward, the microbubbles in the kidney washed out rapidly in comparison with liver or spleen [7]. The enhancement level of some renal lesions was very similar to that of the renal cortex. Therefore, the subjective method of image analysis (i.e., to compare the enhancement of a nodule relative to that of renal cortex) in this study may have some weakness in evaluating the enhancement of this entity; thus, objective methods such as time–intensity curves might be helpful to enhance the performance of image analysis [31]. In this study, the images were analyzed by two readers in consensus and the interobserver reproducibility for CEUS was unknown, thus further studies with independent analysis are necessary to solve this issue. CEUS in kidney may also have some other disadvantages. The image quality of CEUS is influenced by lesion location, bowel gas, ribs, and body configuration of patients, alike what happened for conventional US. Generally, it is difficult to evaluate both kidneys simultaneously with CEUS. CEUS is also an operator-dependent imaging modality and requires sufficient experience [3].

On the basis of the initial experiences, the dynamic blood flow pattern of RCC can be well depicted with the low-MI real-time CEUS technique. Hyper- or iso-enhancement during the cortical phase, subsequent washout in late phase, inhomogeneous enhancement, and perilesional rim-like enhancement are typical CEUS findings for RCCs. Knowledge of these characteristics might be beneficial for improving the diagnosis of RCCs with the use of this enhanced imaging technique.

References

1. Heidenreich A, Ravery V (2004) Preoperative imaging in renal cell cancer. World J Urol 22:307–315
2. Wink MH, de la Rosette JJ, Laguna P, et al. (2007) Ultrasonography of renal masses using contrast pulse sequence imaging: a pilot study. J Endourol 21:466–472
3. Mitterberger M, Pelzer A, Colleselli D, et al. (2007) Contrast-enhanced ultrasound for diagnosis of prostate cancer and kidney lesions. Eur J Radiol 64:231–238
4. Claudon M, Cosgrove D, Albrecht T, et al. (2008) Guidelines and good clinical practice recommendations for the contrast enhanced ultrasound (CEUS)-update 2008. Ultraschall Med 29:28–44
5. Nilsson A (2004) Contrast-enhanced ultrasound of kidneys. Eur Radiol 14(Suppl 8):P104–P109
6. Tamai H, Takiguchi Y, Oka M, et al. (2005) Contrast-enhanced ultrasonography in the diagnosis of solid renal tumors. J Ultrasound Med 24:1635–1640
7. Setola SV, Catalano O, Sandomenico F, et al. (2007) Contrast-enhanced sonography of the kidney. Abdom Imaging 32:21–28
8. Quaia E, Calliada F, Bertolotto M, et al. (2004) Characterization of focal liver lesions with contrast-specific US modes and a sulfur hexafluoride-filled microbubble contrast agent: diagnostic performance and confidence. Radiology 232:420–430
9. Bleuzen A, Tranquart F (2004) Incidental liver lesions: diagnostic value of cadence contrast pulse sequencing (CPS) and SonoVue. Eur Radiol 14:53–62

10. Albrecht T, Blomley M, Bolondi L, et al. (2004) Guidelines for the use of contrast agents in ultrasound. Ultraschall Med 25:249–256
11. Ascenti G, Gaeta M, Magno C, et al. (2004) Contrast-enhanced second-harmonic sonography in the detection of pseudocapsule in renal cell carcinoma. AJR Am J Roentgenol 182:1525–1530
12. Reese JH (1992) Renal cell carcinoma. Curr Opin Oncol 4:427–434
13. Forman HP, Middleton WD, Melson GL, et al. (1993) Hyperechoic renal cell carcinoma: increase in detection at US. Radiology 188:431–434
14. Jinzaki M, Tanimoto A, Narimatsu Y, et al. (1997) Angiomyolipoma: imaging findings in lesions with minimal fat. Radiology 205:497–502
15. Ascenti G, Zimbaro G, Mazziotti S, et al. (2001) Usefulness of power Doppler and contrast-enhanced sonography in the differentiation of hyperechoic renal masses. Abdom Imaging 26:654–660
16. Brannigan M, Burns PN, Wilson SR (2004) Blood flow patterns in focal liver lesions at microbubble-enhanced US. RadioGraphics 24:921–935
17. Isozaki T, Numata K, Kiba T, et al. (2003) Differential diagnosis of hepatic tumors by using contrast enhancement patterns at US. Radiology 229:798
18. Quaia E (2007) Microbubble ultrasound contrast agents: an update. Eur Radiol 17:1995–2008
19. Park BK, Kim B, Kim SH, et al. (2007) Assessment of cystic renal masses based on Bosniak classification: comparison of CT and contrast-enhanced US. Eur J Radiol 61:310–314
20. Ascenti G, Mazziotti S, Zimbaro G, et al. (2007) Complex cystic renal masses: characterization with contrast-enhanced US. Radiology 243:158–165
21. Wang JR, Miao LY, Cui LG, et al. (2008) Application of contrast-enhanced ultrasound in the diagnosis of renal cystic lesion [in Chinese]. Zhongguo Yi Xue Ke Xue Yuan Xue Bao 30:22–26 (in Chinese)
22. Yang B, Fu NH, Shen DJ, et al. (2007) Contrast-enhanced ultrasound in the characteristics of renal tumors. Chin J Ultrasonogr 16:599–601 (in Chinese)
23. Tranquart F, Correas JM, Martegani A, et al. (2004) Feasibility of real time contrast enhanced ultrasound in renal disease. J Radiol 85:31–36
24. Pallwein L, Mitterberger M, Aigner F, et al. (2007) Small renal masses: the value of contrast-enhanced colour Doppler imaging. BJU Int 99:579–585
25. Yamashita Y, Honda S, Nishiharu T, et al. (1996) Detection of pseudocapsule of renal cell carcinoma with MR imaging and CT. AJR Am J Roentgenol 166:1151–1155
26. Pickhardt PJ, Lonergan GJ, Davis CJ, et al. (2000) Infiltrative renal lesions: radiologic-pathologic correlation. RadioGraphics 20:215–253
27. Takahashi S, Ueda J, Furukawa T, et al. (1996) Renal cell carcinoma: preoperative assessment for enucleative surgery with angiography, CT, and MRI. J Comput Assist Tomogr 20:863–869
28. Pretorius ES, Siegelman ES, Ramchandani P, et al. (1999) Renal neoplasm amenable to partial nephrectomy: MR imaging. Radiology 212:28–34
29. Haendl T, Strobel D, Legal W, et al. (2009) Renal cell cancer does not show a typical perfusion pattern in contrast-enhanced ultrasound. Ultraschall Med 30:58–63 (in German)
30. Quaia E, Siracusano S, Bertolotto M, et al. (2003) Characterization of renal tumours with pulse inversion harmonic imaging by intermittent high mechanical index technique: initial results. Eur Radiol 13:1402–1412
31. Li J, Dong BW, Yu XL, et al. (2005) Time–intensity based quantification of vascularity with single-level dynamic contrast-enhanced ultrasonography: a pilot animal study. J Ultrasound Med 24:975–983